Parallel Imaging Reconstruction for Arbitrary Trajectories using k-Space Sparse Matrices (kSPA)

C. Liu[1], R. Bammer[1], and M. E. Moseley[1]

[1]Radiology, Stanford University, Stanford, CA, United States

INTRODUCTION: Despite the recent advances of several parallel imaging algorithms (1, 2, 3, 4), it remains a challenge in many applications to rapidly and reliably reconstruct an image from partially acquired non-Cartesian **k**-space data. Such applications include, for example, 3D imaging, functional MRI (fMRI), perfusion-weighted imaging and diffusion tensor imaging (DTI), where a large number of images have to be reconstructed. In this abstract, we propose a systematic non-iterative reconstruction algorithm termed kSPA that suits arbitrary sampling patterns. The kSPA algorithm computes a sparse approximate inverse that can be applied repetitively to reconstruct all subsequent images. This algorithm is demonstrated using both simulated and *in vivo* data, and the resulting image quality is shown to be comparable to that of the iterative SENSE algorithm (2). In addition, the image reconstruction time can be reduced approximately by a factor of 100 for every thousand images. This algorithm, therefore, is particularly useful for the aforementioned applications.

METHOD: Assuming that the receiving sensitivity of the *n*-th coil has a Fourier transform of $s_n(\mathbf{k}_\rho)$ on a Cartesian grid ($\rho = 1 \cdots N^2$ for an $N \times N$ grid), the data on an arbitrary **k**-space location can be written as,

$$d_n(\boldsymbol{\kappa}_\mu) = \sum_{\rho'=1}^{N^2} m(\mathbf{k}_{\rho'}) \sum_{\rho=1}^{N^2} s_n(\mathbf{k}_\rho - \mathbf{k}_{\rho'})\, c(\boldsymbol{\kappa}_\mu - \mathbf{k}_\rho)\,, \qquad [1]$$

where $c(\mathbf{k}_\kappa)$ is the interpolation kernel. With multiple receiving coils and a number of sampling locations, Eq. [1] forms a system of linear equations that can be denoted as $\mathbf{d} = \mathbf{G}\,\mathbf{m}$. Here, **d** is a column vector stacked with the **k**-space data acquired by all coils; **m** is also a column vector with the **k**-space value to be estimated; **G** is the coefficient matrix. A least-squares solution to this equation is given by

$$\mathbf{m} = (\mathbf{G}^H\mathbf{G})^{-1}\mathbf{G}^H\mathbf{d} = \mathbf{G}^+\mathbf{d}\,. \qquad [2]$$

The matrix $\mathbf{G}^+$ is typically large and can not be computed directly and stored in the memory. To practically solve Eq. [2], we propose to approximate both **G** and $\mathbf{M}^+ = (\mathbf{G}^H\mathbf{G})^{-1}$ as sparse matrixes. The sparse approximation of **G** results from the fact that coil sensitivity is generally a smooth function containing only low spatial frequency components. In other words, the convolution kernel defined by the coil sensitivity is very compact leading to a sparse matrix **G**. The sparse approximation of $\mathbf{M}^+$ is a result of the Cayley-Hamilton theorem. The physical significance of this low-order approximation of $\mathbf{M}^+$ means that a **k**-space sample can be determined by its neighboring samples within a certain distance.

The kSPA algorithm is applied for various **k**-space trajectories including a Cartesian trajectory, a spiral trajectory and a random trajectory. A Shepp-Logan phantom and an 8-channel receiving coil were used to simulate the **k**-space data *via* inverse gridding. *In vivo* brain images of a healthy volunteer were acquired using a spiral readout trajectory on a 1.5T whole-body system (GE Signa, GE Healthcare, Waukesha, WI) equipped with a maximum gradient of 50mT/m and a slew rate of 150 mT/m/s. An 8-channel head coil (MRI Devices Corporation, Pewaukee, WI) was used for image acquisition. The scan parameters were: FOV = 24cm, TR = 4s, TE = 90ms, bandwidth = 125 kHz, and matrix size = 256x256.

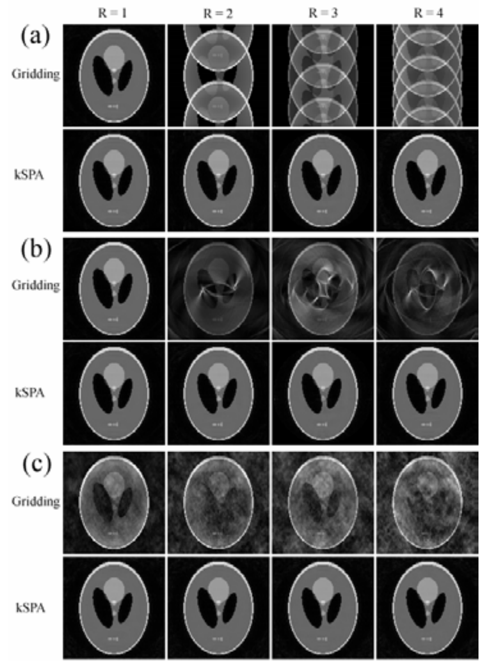

Figure 1 – kSPA reconstruction for three sampling trajectories with undersampling factors up to 4: (a) cartesian, (b) spiral and (c) random trajectory.

RESULTS: Figure 1 compares images reconstructed with gridding and kSPA for all three types of trajectories. Reduction factors range from 1 to 4. The kSPA algorithm results in excellent image quality for all three sampling trajectories. Figure 2 shows the *in vivo* results. The first row shows a typical coil image reconstructed with gridding for each reduction factor, while the second row shows the kSPA images. As expected, the gridding-reconstructed images exhibit severe aliasing artifacts. However, such severe aliasing artifacts are not visible in the kSPA images. For comparison, images reconstructed with SENSE are also shown in Figure 2.

DISCUSSION: We have shown that kSPA is a **k**-space-based parallel imaging reconstruction algorithm that can be applied to arbitrary **k**-space sampling trajectories. While the SENSE algorithm relates the image-domain data with the acquired **k**-space data through a sensitivity-encoded Fourier Transform, kSPA expresses the acquired **k**-space data as a convolution between the spectrum of the coil sensitivity and the spectrum of the image. The kSPA reconstruction, therefore, is a deconvolution process based on undersampled data, which is accomplished by approximating the inverse of the design matrix with a sparse matrix. Its feasibility and accuracy is verified in the simulation study using various undersampling ratios and various trajectories including a Cartesian, a spiral and a random trajectory. *In vivo* studies also showed that the image quality of kSPA is comparable to that of SENSE with a slightly increased computational time for a single image. One favorable property of kSPA is that once $\mathbf{G}^+$ is computed, it can be repetitively applied to reconstruct all other images acquired in the same imaging session. For repetitive image reconstruction, this property offers a significant increase in speed compared to the iterative SENSE approach, which becomes increasingly important for fMRI, DTI and spectroscopic imaging.

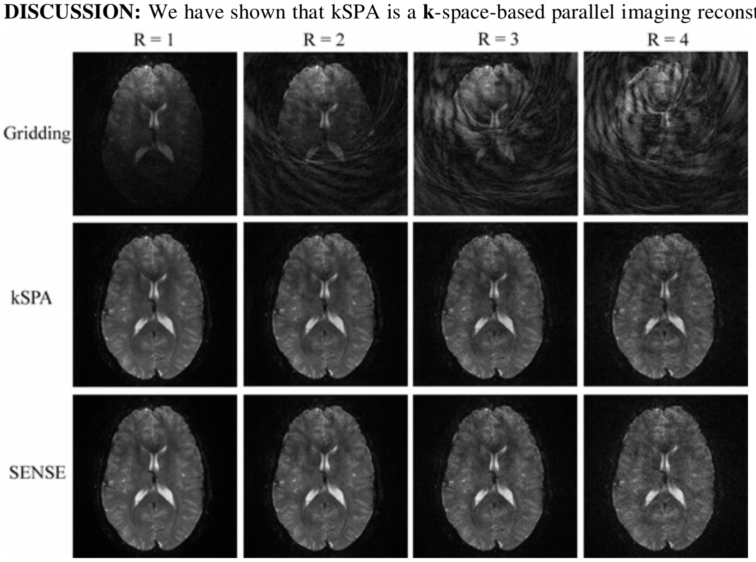

Figure 2 – *In vivo* kSPA reconstruction for spiral sampling with undersampling factors up to 4. The image quality of kSPA is comparable to that of SENSE.

ACKNOWLEDGMENTS: NIH-1R01NS35959, NIH-1R01EB002771, Lucas Foundation, NCRR P41 RR 09784

REFERENCES: 1. Sodickson DK et al. Magn Reson Med 1997;38(4):591-603. 2. Pruessmann KP et al. Magn Reson Med 2001;46(4):638-651. 3. Yeh EN, et al. Magn Reson Med 2005;53(6):1383-1392. 4. Griswold MA, et al. Magn Reson Med 2002;47(6):1202-1210.